Catheterization and Cardiovascular Interventions 82:1075–1082 (2013)

Hemodynamic Impact of Changes in Bifurcation Geometry After Single-Stent Cross-over Technique Assessed by Intravascular Ultrasound and Fractional Flow Reserve

Soo-Jin Kang,[1] MD, PHD, Won-Jang Kim,[1] MD, Jong-Young Lee,[1] MD, Duk-Woo Park,[1] MD, PHD, Seung-Whan Lee,[1] MD, PHD, Young-Hak Kim,[1] MD, PHD, Cheol Whan Lee,[1] MD, PHD, Gary S. Mintz,[2] MD, Seong-Wook Park,[1] MD, PHD, and Seung-Jung Park,[1*] MD, PHD

Background: Angiographic stenosis of a sidebranch (SB) ostium is common after single-stent cross-over, but it is usually not hemodynamically significant. We evaluated the relationship between the mechanisms of SB stenosis and its hemodynamic significance. Methods and Results: We used preinterventional and post-interventional intravascular ultrasound (IVUS) of the main branch (MB) and the SB and post-intervention fractional flow reserve (FFR) of the SB to assess 40 nonleft main bifurcation lesions after a single stent cross-over. Although post-stenting angiographic diameter stenosis >50% was seen in 19 (48%) SB lesions, only 6 (15%) showed FFR < 0.80. Carina shift was seen in all but one lesion; and plaque shift superimposed on the carina shift was found in 18 (45%) lesions. The change in plaque area at the SB ostium positively correlated with preprocedural plaque burden at the carina of distal MB $r = 0.341$, $P = 0.031$). Plaque shift was more common in lesions with FFR < 0.80 vs. ≥0.80 (83% vs. 38%, $P = 0.041$); and FFR < 0.80 was more frequent in lesions with plaque shift superimposed on carina shift versus isolated carina shift (28% vs. 5%, $P = 0.041$). Conclusions: Although carina shift was the main mechanism of SB lumen loss after a single stent cross-over technique, plaque shift superimposed on carina shift appeared to be necessary to cause a hemodynamically significant stenosis (FFR < 0.80). However, post-procedural IVUS assessment did not accurately predict the functional significance. © 2013 Wiley Periodicals, Inc.

Key words: intravascular ultrasound; carina shift; plaque shift; fractional flow reserve

INTRODUCTION

Even though a single stent strategy is preferred for the treatment of coronary bifurcation lesions, angiographic sidebranch (SB) luminal narrowing is frequently observed immediately after main branch (MB) stenting [1–5] However, there is a remarkable discrepancy between angiographic stenosis and physiological significance of the SB lumen loss; and in most cases angiographic SB narrowing post-stent cross-over is not significant when assessed by fractional flow reserve (FFR) [6] Using intravascular ultrasound (IVUS) there are two potential mechanisms of this change in SB ostial geometry, carina shift versus plaque shift [6–11]. While previous studies have suggested that the main mechanisms of angiographic SB narrowing is carina shift, the more important question is the mechanism of hemodynamically significant SB narrowing, that is, a

[1]Department of Cardiology, University of Ulsan College of Medicine, Asan Medical Center, Seoul, South Korea
[2]Cardiovascular Research Foundation, New York, NY

Conflict of interest: Nothing to report.

Grant sponsor: Korea Healthcare Technology Research and Development Project, Ministry of Health and Welfare; grant number: A120711; Grant sponsor: CardioVacular Research Foundation, Seoul, South Korea.

*Correspondence to: Seung-Jung Park, MD, PHD, Department of Cardiology, University of Ulsan College of Medicine, Asan Medical Center, 388-1 Poongnap-dong, Songpa-gu, Seoul, South Korea, 138-736. E-mail: sjpark@amc.seoul.kr

Received 13 August 2012; Revision accepted 7 April 2013

DOI: 10.1002/ccd.24956
Published online 16 April 2013 in Wiley Online Library (wileyonlinelibrary.com).

SB FFR < 0.80 after cross-over stenting. Thus, the main aim of this study is to assess the impact of carina shift versus plaque shift as mechanisms of hemodynamically significant SB lumen compromise after single-stent cross-over in nonleft main bifurcation lesions.

METHODS

Subjects

Between March 2009 and December 2011, we evaluated the patients who had a significant stenosis of a nonleft main bifurcation and underwent drug-eluting stent implantation with a single-stent cross-over or provisional stent strategy. Both MB- and SB-pullback IVUS imaging was performed preprocedure and post-stenting (immediately after MB cross-over stenting) along with post-stenting FFR measurements in the SB. Inclusion criteria were lesions with angiographic diameter stenosis (DS) of the SB ostium $\leq$50% prestenting and distal reference lumen diameter of the SB > 2 mm. We excluded visible thrombus-containing lesions, lesions with predilation of the SB before preprocedural IVUS, and SB balloon inflations at any time before post-stenting SB-pullback IVUS or FFR. Additionally, patients with myocardial infarction, regional wall motion abnormality in either the MB or SB territories, ejection fraction <40%, bypass graft lesions, left main coronary disease, a significant distal lesion within the SB, a significant lesion within the MB proximal to the stented segment, in-stent restenosis, and the inability of the FFR wire to pass lesions in the SB due to tight stenosis or tortuousity. Then, eight patients were excluded because IVUS-imaging catheter failed to cross lesions in the SB through stent struts. Finally, 40 lesions in 40 patients with prestenting and post-stenting IVUS in both the MB and SB–IVUS and post-stenting FFR in the SB were included in the current analysis. The techniques of single-stent cross-over were selected by the operators' decision. Final kissing balloon inflation was considered when the SB had significant stenosis (>50%), decreased FFR (<0.8), deteriorated flow (TIMI grade flow <3) or serious dissection after MB stenting. When the result of final kissing balloon inflation was suboptimal, SB stenting was provisionally performed at the operator's discretion. We obtained written informed consent from all patients, and the ethics committee approved this study.

Angiographic Analysis

Qualitative and quantitative angiographic analysis was done by standard techniques with automated edge-detection algorithms (CAAS-5, Pie-Medical, Netherlands) in the angiographic analysis center of the CardioVascular Research Foundation, Seoul, South Korea [12,13] The Medina classification was used to describe the location and distribution of lesions at the bifurcation [13].

IVUS Imaging and Analysis

IVUS imaging was performed after intracoronary administration of 0.2 mg nitroglycerin using motorized transducer pullback (0.5 mm/s) and a commercial scanner (Boston Scientific/SCIMED, Natick, MA) consisting of a rotating 40 MHz transducer within a 3.2 Fr imaging sheath. Using computerized planimetry (EchoPlaque 3.0, Indec Systems, MountainView, CA), off-line IVUS analysis was performed in the IVUS core laboratory of Asan Medical Center (Seoul, South Korea).

Four segments of the bifurcation were assessed pre-intervention using both MB-pullback and SB-pullback. The carina was identified as the frame immediately distal to the take-off of the side branch [14]. From the MB-pullback the following were identified: (1) MB just distal to the carina, (2) polygon of confluence (confluence zone of MB and SB on longitudinal IVUS image reconstruction in parallel with the angiographic definition suggested by Ramcharitar [15] and modified for IVUS analysis [10,16], and (3) MB just proximal to the polygon of confluence. Separately using the SB pullback, the ostium of the SB just distal to the carina was defined. At the minimal lumen area (MLA) site within each of these four segments, the lumen, stent, plaque plus media (P+M), and external elastic membrane (EEM) areas were measured by 2D-planimetry. Plaque burden was calculated as P+M/EEM $\times$ 100 (%). At the SB carina α was defined as the EEM diameter along the axis through the centers of both the MB and SB lumens, and β was defined as the EEM diameter perpendicular to α. Thus, EEM eccentricity at the SB carina was calculated as [β/α] [10].

Post-stenting, the four segments were identified in parallel with the preprocedural IVUS analysis. Both the minimal stent area within each segment and the stent, lumen, and EEM areas at the SB ostium and carina were measured [10]. The change in MLA within the SB ostium (ΔL), the change in EEM area at the MLA site (ΔV), the change in P+M area at the MLA site (ΔP), and the change in EEM eccentricity were calculated. Carina shift was defined as EEM area reduction (i.e., $\Delta V < 0$) associated with more eccentric change in vessel shape (the change in EEM eccentricity > 0). In contrast, plaque shift was defined as lumen loss greater than the decrease in EEM ($\Delta V/\Delta L < 1$) with a new increase in plaque at the SB ostium (i.e., plaque shift or $\Delta P > 0$).

FFR Measurement

After drug-eluting stent implantation of the MB was performed using the single-stent cross-over technique and before any SB balloon inflations, FFR of the SB was measured. "Equalization" of the two pressures was performed with the guidewire sensor positioned at the guiding catheter tip. Then the 0.014-in pressure guidewire (St. Jude Medical, Minneapolis, MN) was passed through the MB stent struts into the distal SB; and FFR was measured 5 mm distal to the SB ostium at maximal hyperemia induced by intravenous adenosine infusion at 140 μg/kg/min through an antecubital vein. Hyperemic pressure pull-back recordings were performed as described previously. [10,11,17] The SB stenosis was considered functionally significant when the post-stent FFR was <0.80.

Statistical Analysis

All statistical analyses were performed using SPSS (version 10.0, SPSS, Chicago, IL). All values are expressed as the means ± one standard deviation (continuous variables) or as counts and percentages (categorical variables). Continuous variables were compared by use of the nonparametric Mann–Whitney test and Wilcoxon signed-rank tests were used to compare prestenting and post-stenting continuous variables. Categorical variables were compared with the χ^2 statistics or Fisher's exact test. A P value <0.05 was considered statistically significant.

RESULTS

Clinical and Angiographic Findings

The baseline clinical and procedural characteristics in 40 patients are summarized in Table I. The MB was left anterior descending artery in 95% and left circumflex artery in 5%. The SB was 1st diagonal branch in 80%, 2nd diagonal branch in 15%, and obtuse marginal branch in 5%. The quantitative coronary angiographic data are shown in Table II.

Immediately after MB stenting with single-stent cross-over technique, SB FFR was 0.95 ± 0.05 at baseline, and 0.87 ± 0.09 at maximal hyperemia. Although post-stenting DS > 50% was seen in 19 (48%) lesions, only six (15%) lesions showed FFR < 0.80. The FFR had, at most, a modest correlation with the preprocedural DS ($r = -0.306$, $P = 0.055$) or the post-stenting DS ($r = -0.395$, $P = 0.011$) in the SB.

IVUS Predictors of Functional SB Compromise

Table III shows prestenting and post-stenting IVUS findings of both MB and SB. FFR in the SB after MB stenting correlated with the preprocedural MLA ($r = 0.506$, $P < 0.001$), the preprocedural plaque burden ($r = -0.623$, $P < 0.001$), the post-stenting MLA ($r = 0.516$, $P < 0.001$), and the post-stenting plaque burden ($r = -0.675$, $P < 0.001$) within the SB ostium (Fig. 1). FFR in the SB after MB stenting also correlated with the preprocedural lumen area at the carina of the distal MB ($r = 0.397$, $P = 0.011$).

Post-stenting FFR <0.80 was seen in only 5 (31%) of 16 lesions with preprocedural MLA within SB ostium <3.0 mm^2 and in 5 (46%) of 11 lesions with preprocedural MLA within SB ostium <2.5 mm^2. Preprocedural plaque burden >50% was shown in 15 lesions, whereas only five (33%) had post-stenting FFR < 0.80 (Fig. 1). Post-stenting FFR < 0.80 was seen in 6 (24%) of 25 lesions with post-stenting MLA within SB ostium <3.0 mm^2. Even in the 21 lesions with post-stenting MLA within SB ostium <2.5 mm^2,

TABLE I. Baseline Clinical And Procedural Characteristics

Age (years)	59 ± 10
Male, *N* (%)	28 (70%)
Smoking, *N* (%)	10 (25%)
Hypertension, *N* (%)	1 (50%)
Hypercholesterolemia, *N* (%)	15 (38%)
Diabetes mellitus, *N* (%)	7 (18%)
Left ventricular ejection fraction, %	61.7 ± 5.1
Clinical presentation	
Stable angina, *N* (%)	27 (68%)
Unstable angina, *N* (%)	12 (30%)
Acute myocardial infarction, *N* (%)	1 (2%)
Total stent length of MB, mm	27.3 ± 5.3
Maximal balloon pressure (MB), atm	12.8 ± 3.9
Maximal balloon size (MB), mm	3.4 ± 0.3

MB: main branch.

TABLE II. Quantitative Coronary Angiographic Data

Variable	Preprocedural	After MB stenting
Medina classifications		
(1,1,1)	8 (20%)	
(1,1,0)	17 (43%)	
(0,1,1)	2 (5%)	
(1,0,0)	3 (7%)	
(0,1,0)	10 (25%)	
MLD within distal MB, mm	1.5 ± 0.6	2.8 ± 0.4[a]
%DS of distal MB, %	52.2 ± 16.5	6.7 ± 6.3[a]
MLD within proximal MB, mm	1.6 ± 0.5	3.1 ± 0.3[a]
%DS of proximal MB, %	51.9 ± 15.2	7.2 ± 5.2[a]
MLD within SB ostium, mm	1.9 ± 0.4	1.6 ± 0.7[a]
%DS of SB ostium, %	24.8 ± 16.0	42.6 ± 23.2[a]
TIMI 3 at the MB, *N* (%)	40 (100%)	40 (100%)
TIMI 3 at the MB, *N* (%)	40 (100%)	40 (100%)
Angiographic thrombi, *N* (%)	0 (0%)	0 (0%)
Dissection, *N* (%)	0 (0%)	0 (0%)

MLD: minimal lumen diameter, DS: %diameter stenosis.
MB: main branch, SB: sidebranch.
[a]$P < 0.01$ vs. FFR < 0.80.

TABLE III. Intravascular Ultrasound Findings Before and After MB Stenting

	Total ($n=40$)		FFR $<$ 0.80 ($n=6$)		FFR $\geq$ 0.80 ($n=34$)	
	Prestenting	Post-stenting	Prestenting	Post-stenting	Prestenting	Post-stenting
At the distal MB ostium						
Lumen area at the MLA site, mm^2	3.2 ± 1.5	7.3 ± 1.8^a	2.4 ± 0.7	6.0 ± 2.4^a	3.3 ± 1.6	7.5 ± 1.6^a
EEM area at the MLA site, mm^2	9.5 ± 3.5	13.1 ± 3.3^a	7.4 ± 1.8	11.2 ± 3.5^a	9.9 ± 3.6	13.4 ± 3.2^a
Plaque burden at the MLA site, %	64.6 ± 15.3	43.6 ± 9.2^a	66.9 ± 11.1	47.6 ± 7.2^a	64.1 ± 15.9	42.9 ± 9.4^a
Lumen area at carina, mm^2	3.8 ± 1.8	7.6 ± 1.7^a	2.4 ± 0.7	6.3 ± 2.1^a	4.1 ± 1.8^b	$7.9 \pm 1.5^{a,b}$
EEM area at carina, mm^2	10.0 ± 3.8	$13.7 \pm 3.3^*$	7.2 ± 1.9	11.5 ± 3.1^a	10.5 ± 3.8^b	14.1 ± 3.2^a
Plaque burden at carina, %	60.6 ± 14.8	43.3 ± 8.8^a	66.1 ± 10.8	45.7 ± 8.0^a	59.7 ± 15.3	42.8 ± 9.0^a
MLA within the POC, mm^2	4.6 ± 2.6	8.0 ± 1.8	3.6 ± 2.0	6.7 ± 2.2^a	4.8 ± 2.7	$8.3 \pm 1.7^{a,b}$
At the proximal MB ostium						
Lumen area, mm^2	5.0 ± 3.2	8.5 ± 1.6^a	4.2 ± 1.9	7.2 ± 1.4^a	5.2 ± 3.4	$8.8 \pm 1.5^{a,b}$
EEM area, mm^2	13.8 ± 4.4	16.0 ± 3.6^a	11.4 ± 3.1	13.8 ± 3.4^a	14.3 ± 4.5	16.4 ± 3.6^a
Plaque burden, %	64.2 ± 18.2	45.7 ± 8.1^a	63.8 ± 11.8	47.2 ± 7.4^a	64.4 ± 19.3	45.4 ± 8.3^a
At the SB ostium						
Lumen area at the MLA site, mm^2	3.5 ± 1.3	2.8 ± 1.1^a	2.2 ± 0.8	1.6 ± 0.5^a	3.8 ± 1.3^b	$3.0 \pm 1.1^{a,b}$
EEM area at the MLA site, mm^2	6.3 ± 1.9	5.5 ± 1.7^a	5.0 ± 2.1	4.7 ± 1.9	6.6 ± 1.8	5.6 ± 1.6^a
Plaque burden at the MLA site, %	43.4 ± 14.7	48.7 ± 16.1^a	55.5 ± 8.0	65.1 ± 7.0^a	41.2 ± 14.7^b	$45.8 \pm 15.6^{a,b}$
Lumen area at carina, mm^2	3.7 ± 1.6	2.9 ± 1.2^a	2.1 ± 1.1	1.7 ± 0.7	4.0 ± 1.5^b	$3.1 \pm 1.1^{a,b}$
EEM area at carina, mm^2	6.3 ± 2.0	5.6 ± 1.7^a	5.0 ± 2.1	4.7 ± 1.9	6.6 ± 1.8^b	5.6 ± 1.6^a
Plaque burden at carina, %	41.5 ± 15.8	47.9 ± 16.7^a	54.8 ± 9.4	63.9 ± 5.0^a	39.1 ± 15.7^b	$45.0 \pm 16.5^{a,b}$
EEM eccentricity index	1.1 ± 0.1	1.4 ± 0.2^a	1.1 ± 0.1	1.3 ± 0.2	1.1 ± 0.1	1.4 ± 0.2^a

[a] $P < 0.05$, post-stenting vs. prestenting.
[b] $P < 0.05$, FFR $\geq$ 0.80 vs. FFR $<$ 0.80 (nonparametric).
Post-stenting: immediately after MB stenting.
MLA, minimal lumen area; P+M, plaque plus media; EEM, external elastic membrane; POC: polygon of confluence; MB, main branch; SB, side-branch.

only six (29%) had post-stenting FFR $<$ 0.80. Also, six (30%) of 20 lesions with post-stenting plaque burden $>$50% showed post-stenting FFR $<$ 0.80.

Mechanism of SB Stenosis—Carina Shift Versus Plaque Shift

Table IV shows changes of IVUS parameters after MB stenting. After MB stenting, all patients consistently showed a reduction in MLA within the SB ostium and EEM area at the MLA site (Fig. 2); and 31 (78%) patients showed $>$10% MLA loss. In all but one patient, EEM eccentricity increased. The change in EEM eccentricity index correlated with ΔV ($r = -0.400$, $P = 0.011$); and there was a significant correlation between ΔV and ΔL ($r = 0.743$, $P < 0.001$), (Fig. 3). The post-stenting MLA within SB ostium correlated with preprocedural lumen area at the carina of distal MB ($r = 0.351$, $P = 0.026$). Plaque burden at the SB ostium significantly increased after MB stenting (from $43.4 \pm 14.7\%$ to $48.7 \pm 16.1\%$, $P = 0.003$). The change in plaque burden at the SB ostium correlated with the preprocedural lumen area at the carina of the distal MB ($r = -0.319$, $P = 0.045$).

Although the mean value of P+M area did not change significantly, the change in P+M area (ΔP) varied among patients (Fig. 2). While 22 (55%) showed $\Delta P < 0$, the remaining 18 (45%) showed $\Delta P > 0$ with $\Delta P > +10\%$ being observed in 9 (23%) lesions. The ΔP positively correlated with preprocedural plaque burden at the carina of distal MB ($r = 0.341$, $P = 0.031$), but not with the plaque burden of proximal MB ostium ($r = -0.039$, $P = 0.813$) or the plaque burden of the SB ostium ($r = -0.218$, $P = 0.176$).

There was a positive correlation between $\Delta V/\Delta L$ and ΔP ($r = -0.802$, <0.001), (Fig. 4). In 22 (55%) patients isolated carina shift with no plaque shift ($\Delta V/\Delta L \geq 1$ and $\Delta P \leq 0$) was the mechanism of the geometrical change of SB ostium. Conversely, 18 (45%) patients showed $\Delta V/\Delta L < 1$ and $\Delta P > 0$, suggesting plaque shift superimposed on carina shift.

Impact of Geometrical Change of SB on Functional Significance

With regard to the mechanism of hemodynamically significant SB lumen loss, plaque shift was more frequently observed in lesions with FFR $<$ 0.80 in the SB after single-stent cross-over than in those with FFR $\geq$ 0.80 (83% vs. 38%, $P = 0.041$). FFR $<$ 0.80 was seen in five (28%) of 18 lesions with plaque shift superimposed on carina shift, whereas only one (5%) of 22 lesions with isolated carina shift had a post-stent SB FFR $<$ 0.80 ($P = 0.041$).

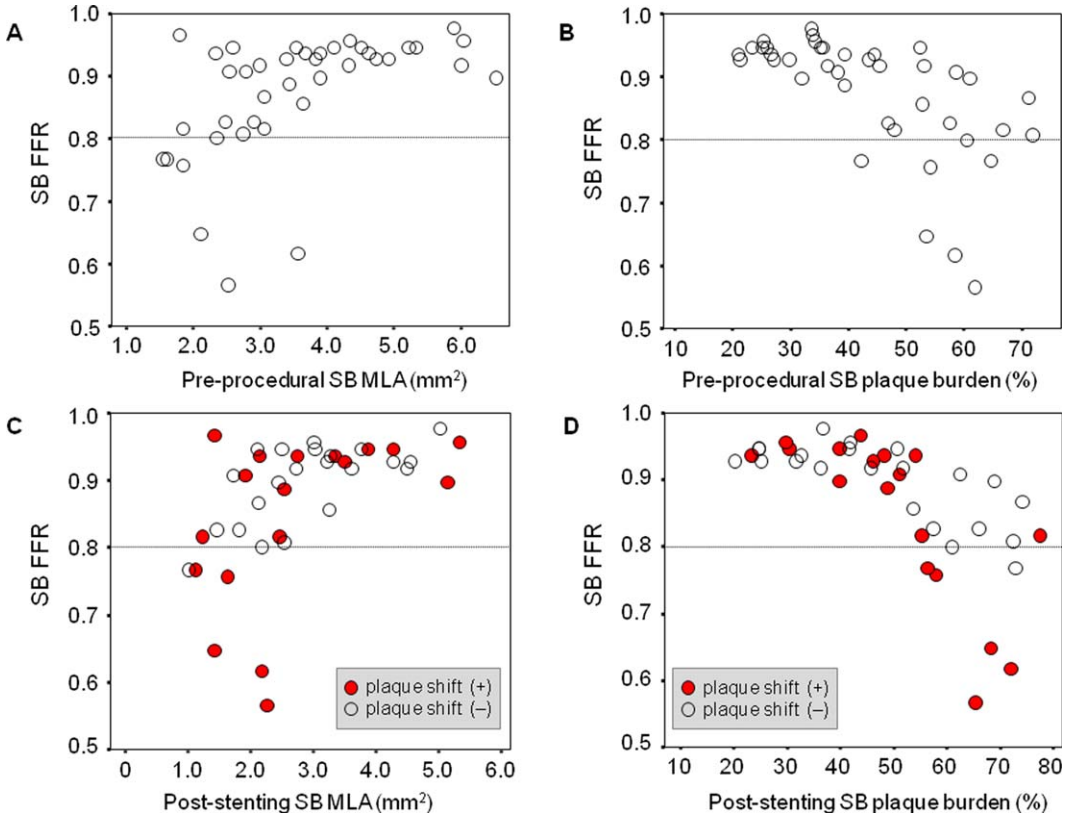

Fig. 1. SB ostial morphology and post-stenting SB FFR. A: Relationship between preprocedural MLA within the SB ostium and post-stenting FFR. B: Relationship between pre-procedural plaque burden within the SB ostium and post-stenting FFR. C: All lesions with post-stenting MLA within SB ostium ≥2.5 mm² had SB FFR ≥ 0.80 after MB stenting, while 6 (29%) of 21 lesions with MLA <2.5 mm² showed FFR < 0.80. D: All lesions with post-stenting SB plaque burden >50% had FFR < 0.80, while 6 (30%) of 20 lesions with plaque burden >50% showed FFR < 0.80. Among the six lesions with FFR < 0.80, 5 (83%) lesions were associated with plaque shift (red circle). [Color figure can be viewed in the online issue, which is available at wileyonlinelibrary.com.]

TABLE IV. Changes of IVUS Parameters After MB Stenting

	Total	FFR < 0.80	FFR ≥ 0.80
N	40	6	34
At the distal MB ostium			
ΔLumen area at the MLA site, mm²	4.1 ± 2.0	3.6 ± 2.1	4.2 ± 2.0
ΔEEM area at the MLA site, mm²	3.6 ± 2.1	3.8 ± 1.9	3.5 ± 2.2
ΔPlaque burden at the MLA site, %	−20.9 ± 12.9	−19.3 ± 12.7	−21.2 ± 13.2
ΔMLA within the POC, mm²	3.4 ± 2.2	3.1 ± 2.4	3.5 ± 2.2
At the proximal MB ostium			
ΔLumen area, mm²	3.5 ± 2.8	3.0 ± 1.8	3.6 ± 2.9
ΔEEM area, mm²	2.2 ± 2.7	2.5 ± 0.7	2.1 ± 2.9
ΔPlaque burden, %	−18.6 ± 18.3	−16.6 ± 15.2	−18.9 ± 19.1
At the SB ostium			
ΔLumen area at the MLA site, mm²	−0.7 ± 0.4	−0.6 ± 0.4	−0.8 ± 0.4
ΔEEM area at the MLA site, mm²	−0.8 ± 0.6	−0.3 ± 0.3	−0.9 ± 0.6*
ΔPlaque burden at the MLA site, %	5.3 ± 4.9	9.6 ± 5.1	4.5 ± 4.5*
ΔLumen area at carina, mm²	−0.8 ± 0.8	−0.4 ± 0.5	−0.9 ± 0.8
ΔEEM area at carina, mm²	−0.7 ± 1.0	−0.0 ± 0.8	−0.8 ± 1.0
ΔPlaque burden at carina, %	6.4 ± 7.1	9.2 ± 6.0	5.8 ± 7.3
ΔEEM eccentricity index	0.2 ± 0.2	0.2 ± 0.2	0.3 ± 0.2

Δ: post-stenting–prestenting
*$P < 0.05$, FFR < 0.80 vs. FFR ≥ 0.80 (nonparametric).

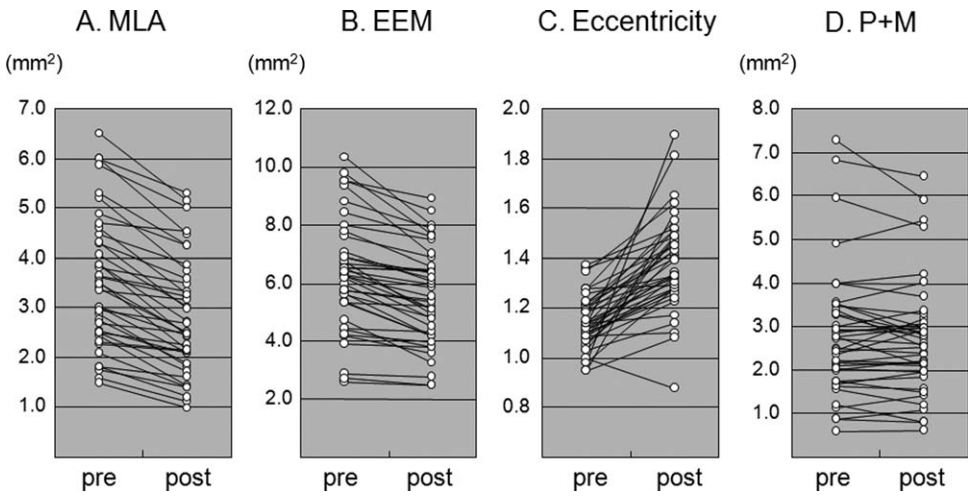

Fig. 2. Geometrical changes in SB ostium after MB stenting. A: prestenting and post-stenting MLA within SB ostium. All patients showed a reduction in MLA after MB stenting (3.5 ± 1.3 mm^2 $\rightarrow$ 2.8 ± 1.2 mm^2, $P < 0.001$). B: A decrease in EEM area was found in all patients (6.3 ± 1.9 mm^2 $\rightarrow$ 5.5 ± 1.7 mm^2, $P<0.001$). C: EEM eccentricity index increased after MB stenting (1.1 ± 0.1 $\rightarrow$ 1.4 ± 0.2, $P < 0.001$). D: P+M areas were not significantly changed(2.8 ± 1.5 mm^2 $\rightarrow$ 2.7 ± 1.3 mm^2, $P = 0.215$),

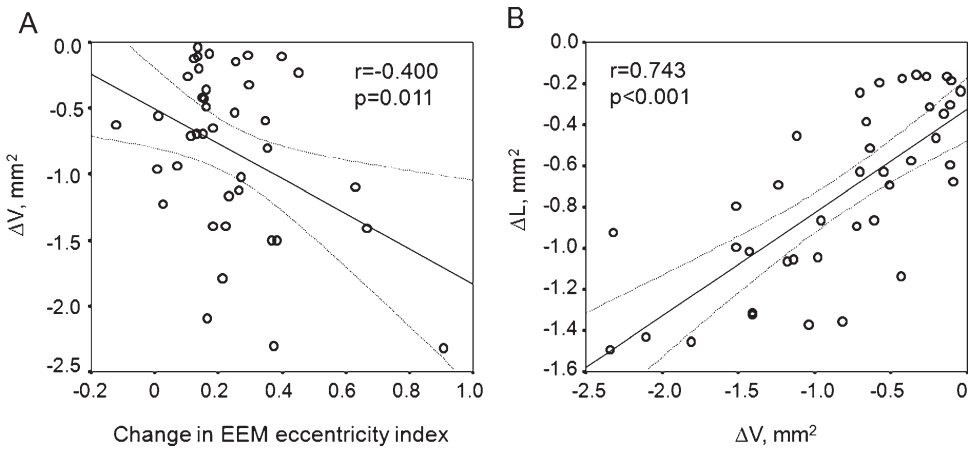

Fig. 3. A: Correlation between the change in EEM eccentricity index and the change in EEM area (ΔV) of SB ostium. B: Correlation between the change in EEM area (ΔV) and the change in MLA (ΔL) of SB ostium

DISCUSSION

The major findings of this study are summarized as follows. (1) In nonleft main bifurcation lesions with SB DS <50% preprocedure, the incidence of functional SB compromise post-stenting was only 15%. (2) The small prestenting and post-stenting MLA within the SB ostium could not predict post-stenting FFR < 0.80. (3) Carina shift was the most common mechanism of anatomic ostial SB lumen loss after single-stent crossover; however, in the subset with functional SB compromise, plaque shift appeared to play the more important role.

Anatomic Predictors of Functionally Significant SB Ostial Lumen Compromise

Previous studies reported that only 20–27% of SB lesions with post-stenting DS >70–75% had FFR < 0.75 [6,8,18]. Consistently, our current study demonstrated that 68% of the SB with angiographically significant stenosis (DS >50%) showed normal FFR. In the current study ~30% of the lesions with a small post-stenting MLA within SB ostium <2.5 mm^2 or a large post-stenting plaque burden >50% showed post-stenting FFR < 0.80.

Our previous analysis in 90 nonleft main bifurcation lesions suggested that preprocedural MLA within the

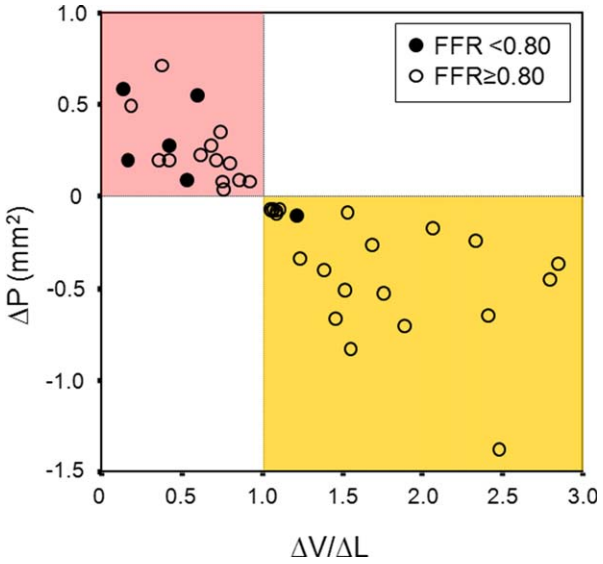

Fig. 4. Positive correlation between ΔV/ΔL and ΔP. Isolated carina shift defined as ΔV/ΔL < 1 and ΔP ≥ 0 was seen in 22 (55%) lesions (yellow area), while plaque shift defined as ΔV/ΔL < 1 and ΔP > 0 was associated in 18 (45%) lesions (red area). [Color figure can be viewed in the online issue, which is available at wileyonlinelibrary.com.]

SB ostium <2.4 mm^2 (sensitivity 94%, specificity 69%) and the plaque burden ≥51% (sensitivity 75%, specificity 71%) predicted post-stenting FFR < 0.80 [9]. With the lower PPV <50%, functional significance of jailed SB could not be reliably predicted by either preprocedural or postprocedural angiography or IVUS.

Mechanisms of Functionally Significant SB Compromise

Almost all of our nonleft main bifurcation lesions showed carina shift characterized by a reduction in ostial SB vessel and lumen area and a more eccentric vessel shape after cross-over main vessel stenting. Conversely, less than a half of the lesions showed plaque shift superimposed on carina shift, as indicated by lumen loss of the SB ostium that was greater than the reduction in vessel area with new plaque gain at the SB ostium. Although our previous study reported similar findings in left main bifurcations, lack of functional evaluation (i.e., FFR) limited the assessment of the hemodynamic impact of the changes in SB ostial geometry [10]. Previous inferential data showed similar results in non-LM bifurcation lesions; the sidebranch was not studied directly, but morphological changes were assessed by changes in MB segments as a surrogate [8]. By directly comparing prestenting and post-stenting SB-IVUS images, the current study clarified the changes in SB geometry and their relation to functional significance.

There appears to be a significant difference between the mechanisms of anatomically significant, but functionally insignificant SB compromise versus SB compromise with an FFR < 0.80 after main vessel stenting. Our data suggests that plaque shift may be required in order to get functional SB compromise. Thus, while carina shift is seen in most bifurcation lesions and is responsible for anatomic changes in both left main and nonleft main locations, it seems that plaque shift—whether or not superimposed on carina shift—may be more important hemodynamically.

A previous angiographic study reported that the minimal lumen diameter of the MB distal to the carina independently predicted SB FFR after MB stenting [8]. Similarly, our data showed a negative correlation between preprocedural lumen area at the distal MB carina and post-stenting SB FFR. We found that a smaller lumen area at the MB carina was related to a greater increase in SB plaque burden leading to a smaller lumen area and functional significance at the SB ostium. Even though a functional SB stenosis was mainly determined by disease of SB ostium preprocedure, severe disease at the MB carina may also contribute to plaque shift and a functionally significant SB stenosis.

Limitations

First, the current study evaluated selected lesions with preprocedural angiographic DS <50%. Second, post-stenting SB assessment by SB-pullback IVUS could not be performed in all cases. Third, carina angle was not assessed by quantitative coronary angiography or other imaging modalities. Fourth, the number of hemodynamically significant SB ostial stenosis was small. Fifth, The FFR cutoff values between 0.75 and 0.80 have been generally used. Although a previous study suggested SB FFR > 0.75 as a safe cut-off for deferral [6]. We used the upper limit 0.80 in this analysis to completely exclude ischemia-inducing lesions. The optimal IVUS cut-off value predicting post-stenting FFR was not provided due to small sample size and small number of the cases with functional compromise. Finally, long-term clinical impact of the geometrical change in SB ostium and its hemodynamic significance were not addressed.

CONCLUSIONS

Functional SB compromise was less common than anatomical stenosis and could not be predicted by anatomic parameters, whether assessed preintervention or post-intervention. Although carina shift was a general mechanism of anatomic SB lumen loss, plaque

shift was more likely associated with functional SB compromise.

REFERENCES

1. Colombo A, Bramucci E, Saccà S, Violini R, Lettieri C, Zanini R, Sheiban I, Paloscia L, Grube E, Schofer J, Bolognese L, Orlandi M, Niccoli G, Latib A, Airoldi F. Randomized study of the crush technique versus provisional side-branch stenting in true coronary bifurcations: The CACTUS (Coronary Bifurcations: application of the Crushing Technique Using Sirolimus-Eluting Stents) Study. Circulation 2009;119:71–78.
2. Steigen TK, Maeng M, Wiseth R, Erglis A, Kumsars I, Narbute I, Gunnes P, Mannsverk J, Meyerdierks O, Rotevatn S, Niemelä M, Kervinen K, Jensen JS, Galløe A, Nikus K, Vikman S, Ravkilde J, James S, Aarøe J, Ylitalo A, Helqvist S, Sjögren I, Thayssen P, Virtanen K, Puhakka M, Airaksinen J, Lassen JF, Thuesen L, Nordic PCI Study Group. Randomized study on simple versus complex stenting of coronary artery bifurcation lesions: The Nordic Bifurcation Study. Circulation 2006;114:1955–1961.
3. Ferenc M, Gick M, Kienzle RP, Bestehorn HP, Werner KD, Comberg T, Kuebler P, Büttner HJ, Neumann FJ. Randomized trial on routine vs provisional T-stenting in the treatment of de novo coronary bifurcation lesions. Eur Heart J 2008;29: 2859–2867.
4. Colombo A, Moses JW, Morice MC, Ludwig J, Holmes DR Jr, Spanos V, Louvard Y, Desmedt B, Di Mario C, Leon MB. Randomized study to evaluate sirolimus-eluting stents implanted at coronary bifurcation lesions. Circulation 2004;109: 1244–1249.
5. Tanabe K, Hoye A, Lemos PA, Aoki J, Arampatzis CA, Saia F, Lee CH, Degertekin M, Hofma SH, Sianos G, McFadden E, Smits PC, van der Giessen WJ, de Feyter P, van Domburg RT, Serruys PW. Restenosis rates following bifurcation stenting with sirolimus-eluting stents for de novo narrowings. Am J Cardiol 2004;94:115–118.
6. Koo BK, Park KW, Kang HJ, Cho YS, Chung WY, Youn TJ, Chae IH, Choi DJ, Tahk SJ, Oh BH, Park YB, Kim HS. Physiological evaluation of the provisional side-branch intervention strategy for bifurcation lesions using fractional flow reserve. Eur Heart J 2008;29:726–732.
7. Vassilev D, Gil R. Clinical verification of a theory for predicting side branch stenosis after main vessel stenting in coronary bifurcation lesions. J Interv Cardiol 2008;21:493–503.
8. Koo BK, Waseda K, Kang HJ, Kim HS, Nam CW, Hur SH, Kim JS, Choi D, Jang Y, Hahn JY, Gwon HC, Yoon MH, Tahk SJ, Chung WY, Cho YS, Choi DJ, Hasegawa T, Kataoka T, Oh SJ, Honda Y, Fitzgerald PJ, Fearon WF. Anatomic and functional evaluation of bifurcation lesions undergoing percutaneous coronary intervention. Circ Cardiovasc Interv 2010;3:113–119.
9. Kang SJ, Mintz GS, Kim WJ, Lee JY, Park DW, Lee SW, Kim YH, Lee CW, Park SW, Park SJ. Preintervention angiographic and intravascular ultrasound predictors for side branch compromise after a single-stent crossover technique. Am J Cardiol 2011;107:1787–1793.
10. Kang SJ, Mintz GS, Kim WJ, Lee JY, Oh JH, Park DW, Lee SW, Kim YH, Lee CW, Park SW, Park SJ. Changes in left main bifurcation geometry after a single-stent crossover technique: An intravascular ultrasound study using direct imaging of both the left anterior descending and the left circumflex coronary arteries before and after intervention. Circ Cardiovasc Interv 2011;4:355–361.
11. Gil RJ, Vassilev D, Formuszewicz R, Rusicka-Piekarz T, Doganov A. The carina angle-new geometrical parameter associated with periprocedural side branch compromise and the long-term results in coronary bifurcation lesions with main vessel stenting only. J Interv Cardiol 2009;22:E1–E10.
12. Ryan TJ, Faxon DP, Gunnar RM, Kennedy JW, King SB 3rd, Loop FD, Peterson KL, Reeves TJ, Williams DO, Winters WL Jr. Guidelines for percutaneous transluminal coronary angioplasty. A report of the American College of Cardiology/American Heart Association Task Force on assessment of diagnostic and therapeutic cardiovascular procedures (subcommittee on percutaneous transluminal coronary angioplasty). Circulation 1988;78:486–502.
13. Medina A, Suárez de Lezo J, Pan M. A new classification of coronary bifurcation lesions. Rev Esp Cardiol 2006;59:183.
14. Rodriguez-Granillo GA, García-García HM, Wentzel J, Valgimigli M, Tsuchida K, van der Giessen W, de Jaegere P, Regar E, de Feyter PJ, Serruys PW. Plaque composition and its relationship with acknowledged shear stress patterns in coronary arteries. J Am Coll Cardiol 2006;47:884–885.
15. Ramcharitar S, Onuma Y, Aben JP, Consten C, Weijers B, Morel MA, Serruys PW. A novel dedicated quantitative coronary analysis methodology for bifurcation lesions. EuroIntervention 2008;3:553–557.
16. Kang SJ, Mintz GS, Kim WJ, Lee JY, Park DW, Yun SC, Lee SW, Kim YH, Lee CW, Han KH, Kim JJ, Park SW, Park SJ. Impact of intravascular ultrasound findings on the long-term repeat revascularization in patients undergoing drug eluting stent implantation for severe unprotected left main bifurcation narrowing. Am J Cardiol 2011;107:367–373.
17. Pijls NH, De Bruyne B, Peels K, Van Der Voort PH, Voort PH, Bonnier HJ, Bartunek J, Koolen JJ, Measurement of fractional flow reserve to assess the functional severity of coronary artery stenoses. N Engl J Med 1996;334:1703–1708.
18. Koo BK, Kang HJ, Young TJ, Chae IH, Choi DJ, Kim HS, Sohn DW, Oh BH, Lee MM, Park YB, Choi YS, Tahk SJ. Physiologic assessment of jailed side branch lesions using fractional flow reserve. J Am Coll Cardiol 2005;46:633–637.